International Journal of Integrated Engineering: Special issue 2018:
Mechanical Engineering, Vol. 10 No. 5 (2018) p. 1-7
© Penerbit UTHM
DOI: https://doi.org/10.30880/ijie.2018.10.05.001

# Entropy-Based Approach for Fatigue Crack Growth Rate of Dual-Phase Steel

**R. Idris, S. Abdullah*, P. Thamburaja, M. Z. Omar**

Centre for Integrated Design for Advanced Mechanical System (PRISMA), Faculty of Engineering and Built Environment, Universiti Kebangsaan Malaysia, 43600 UKM Bangi, Selangor, Malaysia.

Received 19 April 2018; accepted 12 September 2018, available online 30 October 2018

**Abstract:** This paper presents an entropy-based approach for the fatigue crack growth of dual-phase steel under a constant amplitude loading. According to the degradation-entropy generation theorem, the degradation coefficient can be derived from the correlations of entropy and crack propagation. The temperature evolutions induced for the duration of the fatigue crack growth tests on the as-received and dual-phase steel till it failed were measured to ensure their validity. The results of the present model and the calculated Paris-regime crack growth data were analysed to reach the conclusion that the temperature at the surface of a specimen during a fatigue crack growth test can be used for the assessment of fatigue crack growth by the intensity of the degradation coefficient. The predicted results showed that the present model could accurately predict the fatigue crack growth rate of dual-phase steel with a regression value ($R^2$) of 0.9952.

**Keywords:** Degradation-entropy generation theorem, Dual-phase steel, Entropy generation, Fatigue crack growth rate.

## 1. Introduction

The fatigue process is often followed by an energy transformation, and it is practical to aim at designing a thermodynamic framework by considering its characteristics. Generally, energy dissipation is an irreversible process that establishes the concept of thermodynamic entropy production as a perfect tool for designing its behaviour [1]. As mentioned by the second law of thermodynamics, every dissipative process is accompanied by an increase in entropy, e.g. twinning, plasticity, grain boundary motion, phase transformation [2, 3], etc. Besides that, entropy production has been utilized as a way of measuring the degradation of a component, for example, wear and friction [4], as well as damage accumulation as a consequence of fatigue. Other researchers have recommended the calculation of the entropy generation during the low-cycle fatigue of metals within their experimental methods together with its theoretical formulation [5, 6]. Moreover, the crack layer concept has also been produced to understand the evolution of damage along with the active zone having a crack layer within the fatigue loading histories together with the achievement of a crack layer constitutive relationship [7]. Additionally, the crack growth rates are well correlated with the dissipated energy regardless of the plane stress or plane strain [8].

Fatigue is supposed to be the most frequent source of structural degradation and most of the failure that occur in engineering began with cracks [9], thereby making the accurate prediction of fatigue significantly essential for sustaining safety in engineering systems. Degradation or aging is related to entropy generation, which typically accumulates gradually and decreases the performance of a device until its final failure. The relationship between the irreversible processes of degradation and entropy generation that occur within a system have been established [10]. The fundamental understanding that entropy monotonically increases and free energy monotonically decreases for each natural process such that an entropy-generating irreversible process comes with all aging processes has always been viewed as the driving motivation in relation to the creation of the Degradation-Entropy Generation (DEG) theorem. In implementing the approach of entropy increase, manufactured components change to their natural condition by means of degradation, which generally decreases the integrity of the material properties and finally, renders the components non-functional [11]. To the best of the authors' knowledge, the entropy generated from crack propagation represents an aspect that has typically not been completely studied yet throughout the framework of fracture mechanics. Thus, it would be of great significance to study the fatigue crack growth (FCG) rate based on the entropy approach.

In the present study, efforts were made to prove that fatigue degradation and entropy generation are correlated, thereby ensuring that their relationship would be evaluated for use in the prediction of the

*Corresponding author: shahrum@ukm.edu.my
2011 UTHM Publisher. All right reserved.

FCG rate, according to the DEG theorem, and to fundamentally enhance the studies referring to the FCG rate while avoiding having to look for conventional methods that are dependent on empirical models. The predictive FCG rate, from the evaluation of the fatigue degradation and entropy generation, and the results showed that the concept of the DEG theorem is a reliable method for predicting the FCG rate.

## 2. Degradation-Entropy Generation Theorem

The DEG theorem involving cyclic fatigue was developed by Bryant et al. [12]. According to the DEG theorem, only one dissipative process, $p$ is responsible for causing degradation in a system for entropy generation. It is assumed that $w$ indicates a measure of the degradation of the system and that it is dependent upon the dissipative process, given that $w = w(p)$. Equivalent to the entropy generation, the degradation rate, $D = dw/dt$ can be achieved by employing the chain rule as:

$$D = \frac{dw}{dt} = \left(\frac{\partial w}{\partial p}\frac{\partial p}{\partial \zeta}\right)\frac{\partial \zeta}{\partial t} = YJ \tag{1}$$

where, $Y = \frac{\partial w}{\partial p}\frac{\partial p}{\partial \zeta}$ and $J = \frac{\partial \zeta}{\partial t}$. Together with the thermodynamic force, Bryant et al. [12] related $Y$ to be the degradation force. It can be observed that the degradation of the system relies on the same dissipative process, $p$ as does the entropy generation. Given that the thermodynamic flow, $J$ is probably the common parameter in Equation (1), a degradation coefficient might be known as:

$$B = \frac{Y}{X} = \frac{(\partial w/\partial p)(\partial p/\partial \zeta)}{(\partial_i s/\partial p)(\partial p/\partial \zeta)} = \left|\frac{\partial w}{\partial_i s}\right| \tag{2}$$

where $B$ determines exactly how the entropy generation and degradation relate to the level of the dissipative process, $p$.

In the present study, the crack growth was assumed to occur at a stable rate. The crack length was defined as the degradation parameter, that is, $w = a$, in Equation (1). Consequently, the degradation could well be considered as $a = a\{W_p(N)\}$, where the plastic energy generation at the crack tip, $W_p$, was probably the main dissipative process by having the number of cycles, $N$ to be the phenomenological variable. Based on Equation (1), it can simply be written that $da/dt = YJ$, where $J = dN/dt$ and $Y = \left(da/dW_p\right)x\left(dW_p/dN\right)$. By assuming that the plastic energy is dissipated as entropy generation, that is, $dW_p = Td_i s$, hence, the entropy generation can easily be indicated as:

$$\sigma = \frac{d_i s}{dt} = \frac{\partial_i s}{\partial p}\frac{\partial p}{\partial N}\frac{\partial N}{\partial t} = \frac{f}{T}\frac{dW_p}{dN} \tag{3}$$

where $f$ is the test frequency. By applying $X = (1/T)(dW_p/dN)$ into Equation (1), the following is obtained:

$$D = \frac{da}{dt} = YJ = BXJ = B\frac{f}{T}\frac{dW_p}{dN} \tag{4}$$

The degradation coefficient, $B$ in Equation (4) determines exactly how the entropy generation and crack growth are related to the level of dissipative plastic deformation.

A method to deduce the Paris law of crack growth was developed to assess the energy dissipation in the plastic zone ahead of the crack tip, $W_p$, by using a correlation presented by Klingbeil [13]:

$$\frac{dW_p}{dN} = At\frac{(\Delta K)^4}{\mu\sigma_y^2} \tag{5}$$

where $A$ is a dimensionless constant, $\Delta K$ is the stress intensity factor, $t$ is the specimen thickness, $\sigma_y$ is the yield stress, and $\mu$ is the shear modulus. Substituting Equation (5) into Equation (4) gives:

$$\frac{da}{dN} = \frac{da}{fdt} = B\frac{At}{T}\frac{(\Delta K)^4}{\mu\sigma_y^2} = C(\Delta K)^4 \tag{6}$$

Equation (6) represents the Paris-Erdogan law of crack growth with a constant $C$, defined as:

$$C = B\frac{At}{T\mu\sigma_y^2} \tag{7}$$

Equation (7) indicates the interaction between the constant, $C$ in the Paris-Erdogan law and the degradation coefficient, $B$ that is consequently associated with entropy generation.

## 3. Material and Experimental Procedure

The material used for this investigation was low-carbon steel. The chemical composition of this steel was obtained through the Glow Discharge Spectrometer, (GDS) test and its results are shown in Table 1. The as-received steel was first heated up to inter-critical annealing temperatures in the (ferrite + austenite region), which is 800 °C, for 90 minutes, followed by rapid cooling (water quenching) to produce a dual-phase steel. Finally, the tempering treatment was performed at 400 °C, with a holding time of 2 hours, and then, cooled to room temperature to remove residual stress and to enhance toughness.

Table 1 Chemical composition of the steel, wt (%).

| Elements | wt (%) |
|---|---|
| C | 0.192 |
| Mn | 1.61 |
| Si | 0.384 |
| P | 0.0162 |
| S | 0.0085 |
| Al | 0.0314 |

FCG tests were carried out on a servo-hydraulic universal test machine with a 100-kN capacity load cell using compact tension (CT) specimens, according to ASTM E647. Fig. 1 (a) shows the geometry of the CT specimens with a width (W) of 50 mm, and thickness (B) of 12 mm. Each CT specimen was subjected to a fatigue pre-cracking process in order to initiate a crack and to provide a sharpened fatigue crack of a suitable size and straightness before the FCG rate tests were performed by employing a maximum stress intensity factor, $K_{max}$ set to 32 MPa.m$^{1/2}$. In the present study, the pre-crack length of 0.10B (1.2 mm) was made for each CT specimen. All the FCG tests were conducted in air at room temperature using a constant amplitude sinusoidal waveform loading with a selected load ratio of R = 0.1 at a frequency of 10 Hz until the specimen fractured [14, 15]. The crack length measurement was performed by using the compliance method according to ASTM E647 by employing a clip gauge at the notch mouth. A thermocouple was used to record the temperature evolution of the specimen during the entire test. Additionally, a high-speed, high-resolution infrared (IR) thermal imager was used to calibrate the thermocouple to decrease the error in the prediction of the entropy generation, mostly at the start of the FCG test. Fig. 1 (b) shows the experimental setup for the FCG test.

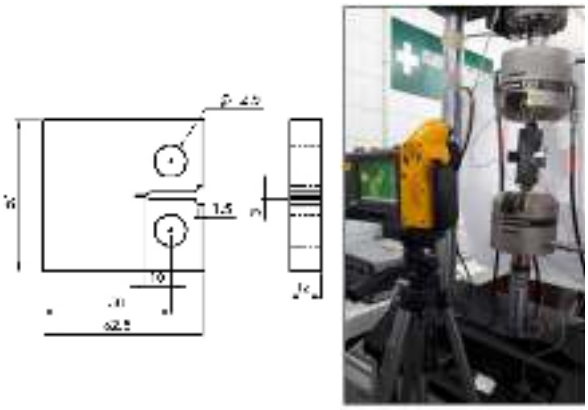

(a) (b)

Fig. 1 (a) Specimen geometry used for FCG testing (all dimensions are in mm); (b) Experimental setup for FCG test.

## 4. Results and Discussion

FCG tests were performed under a constant amplitude loading for the as-received and dual-phase steel specimens. All the tests were conducted until fracture occurred to determine the FCG rate by using the entropy approach.

### 4.1 Temperature Evolution

A typical temperature evolution was plotted as a function of the number of cycles for the as-received and dual-phase steel specimens during the entire FCG test under constant amplitude loading (CAL) conditions, as indicated in Fig. 2. The information in Fig. 2 reveals that the temperature evolution experienced three distinct phases [16]. During the first stage, the temperature at the surface of the specimen increased rapidly at the beginning of the test following the reaction of the material to unpredicted movements, defects and dislocations, and in association with the surface intrusion and extrusion. Then, at the second stage, the temperature levelled off and became steady, but began to rise suddenly just before the occurrence of failure, which was the third stage.

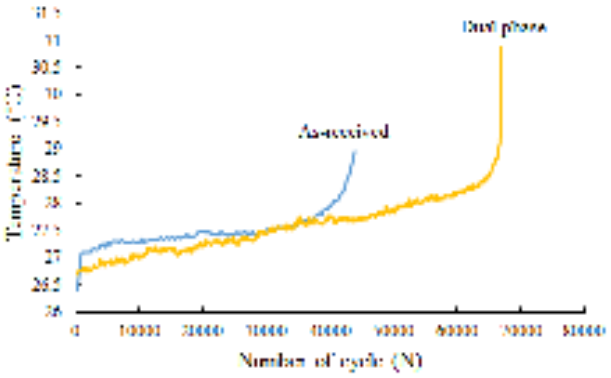


Fig. 2 Typical temperature evolution of the steels.

### 4.2 Fatigue Crack Growth under Cyclic Loading

The FCG process is often classified into three stages, namely, the slow growing region (stage I), the stable growing region (stage II), and the rapidly growing region (stage III). Other researcher found that the deeper the cracks with shorter crack width are accomplished to reduce the fatigue crack growth rate [17].Fig. 3 shows the fatigue life of the as-received and dual-phase steels based on the crack length measurement during the FCG test. This figure showed that the crack initially grew at a slow rate and started to accelerate as the crack length increased after passing through many cycles. The final point for each curve was represented by means of the final fracture through the FCG testing. It could be seen that the analysis of FCG for the dual-phase steel endured the longest life at 66,867 cycles, while the as-received steel had the shortest life at 43,910 cycles. This showed that the fatigue life of the dual-phase steel

was longer than the fatigue life of the as-received steel due to the existence of a harder second phase, namely, martensite, in the dual-phase steel [18].

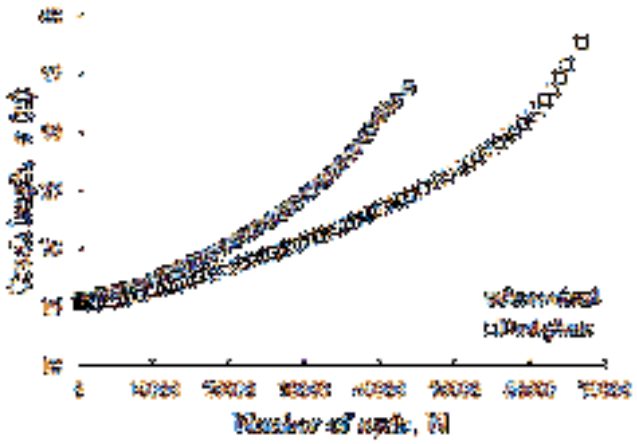

Fig. 3 Fatigue life of steels based on crack length observations.

## 4.3 Entropy Generation

The total entropy generation was obtained from the beginning of the FCG test until the occurrence of fracture ($N_f$), and it was calculated as shown below [5]:

$$S_f = \int_0^{N_f} \left( \frac{E_d}{T} \right) dN \tag{8}$$

where $S_f$ is the total entropy generation of a fatigue failure, $E_d$ is the energy dissipated, $T$ is the surface temperature of the specimen and $N$ is the number of loading cycles.

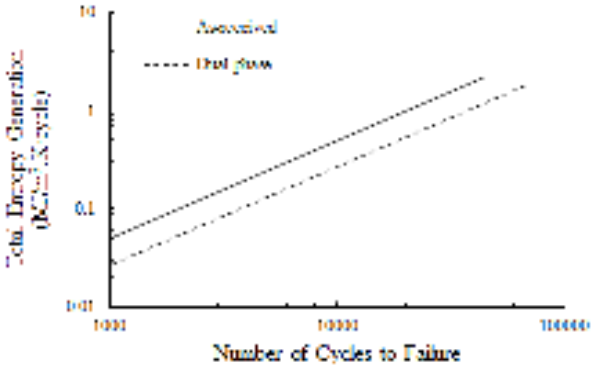


Fig. 4 Evolution of total entropy generation.

Fig. 4 shows the results of the total entropy generation for the dual-phase and as-received steel going through cyclic loading up until failure occurred. The total entropy generation was set to zero at the beginning of the test. Then, it linearly increased until after it achieved failure. It was observed that the as-received steel consumed the total entropy generation of 2.16 MJ/m$^3$.K, while for dual-phase steel, the total entropy generation was 1.77 MJ/m$^3$.K. The difference in the values of the total entropy generation between the as-received and dual-phase steel was due to changes in the total energy dissipated for each material. Besides that, the fatigue life of each specimen was different due to differences in the FCG mechanism resulting from different microstructures.

## 4.4 Degradation Rate Parameter

As stated earlier, the crack length was assumed to be the degradation parameter, $w = a$. The relationship between the rate of entropy generation and the rate of degradation in relation to the degradation coefficient, $B$ for the as-received and dual-phase steel are shown in Fig. 5 and Fig. 6, respectively. It clearly illustrated that for the degradation rate for this study, the crack length, $da/dN$, which was regarded as the degradation parameter, had a linear relationship with the parts of entropy generation, $da/dN = B\sigma$. It was determined that the degradation coefficient, $B$ for the dual-phase steel was smaller than the degradation coefficient, $B$ for the as-received steel. This was probably due to the sub-grain arrangement, which was actually attributed to the martensitic lath structure during the tempering process. Moreover, the steel, which was subjected to the tempering process at a high temperature, improved the rearrangement since the sub-grain structure along the grain boundaries would have been the potential reason for the early failure and the resultant loss in rupture strength [19].

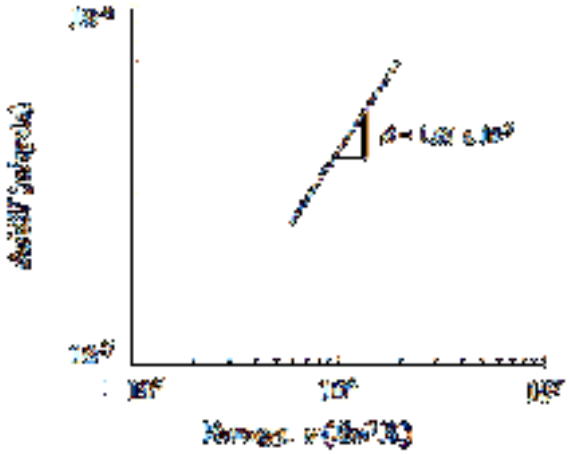

Fig. 5 Relationship between rate of degradation parameter and the entropy generation for as-received steel.

## 4.5 Estimation of Fatigue Crack Growth Rate

The comparison between the estimated FCG rate, $da/dN$ vs $\Delta K$ using Equation (6) and the experimental results are shown in Fig. 7 and Fig. 8 for the as-received as well as dual-phase steel specimens,

respectively. The results encouraged the understanding between the present model and the experimental results. In the present study, the dual-phase steel was known to have $\Delta K^{3.26}$, which was nearest to $\Delta K^4$ when compared to that of the as-received steel, which was $\Delta K^{1.51}$. A statistical test of the variance in providing residuals, i.e. the root mean square error (RMSE), was applied to determine the accuracy of the present model with regard to the experimental data. Table 2 indicates the RMSE results for the as-received and dual-phase steels. The results showed that the present model was able to accurately predict the measured crack growth data for the material, where $\Delta K$ was very closely scaled with $\Delta K^4$. Hence, it was determined that this model was sensitive to differences in the FCG mechanism as a result of the different microstructures of the given material.

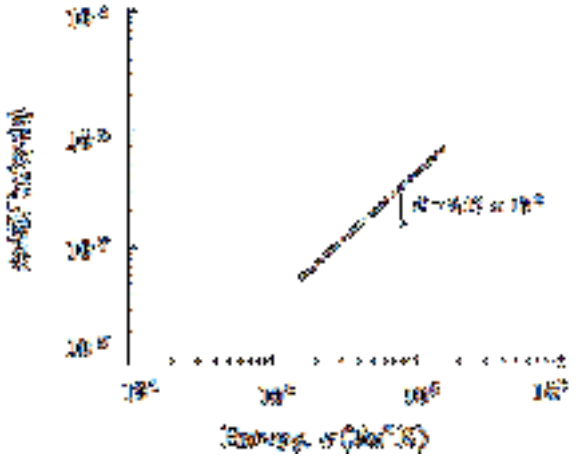

Fig. 6 Relationship between rate of degradation parameter and the entropy generation for dual-phase steel.

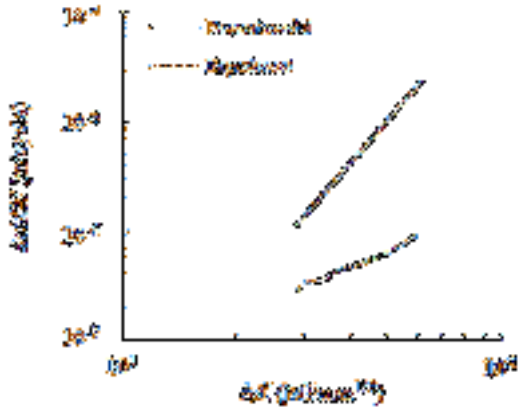

Fig. 7 Comparison of the predicted crack growth rate using present model with experimental data for as-received steel.

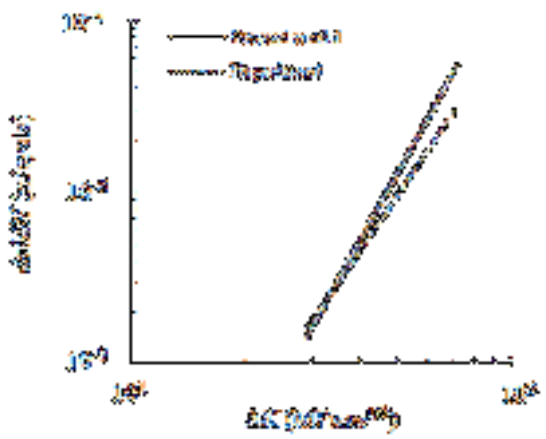

Fig. 8 Comparison of the predicted crack growth rate using present model with experimental data for dual-phase steel.

Table 2 The accuracy of the present model with respect to the experimental data.

| Material | RMSE (m/cycle) |
|---|---|
| As-received | $2.0836 \times 10^{-5}$ |
| Dual-phase | $7.3471 \times 10^{-7}$ |

Fig. 9 and Fig. 10 show the correlation between the predicted FCG rate using the present model and the calculated FCG rate from the experimental data. The regression value, $R^2$ for the as-received steel was 0.8759, while for the dual-phase steel it was 0.9952. The regression value that was obtained indicated that the predicted FCG rate fitted well for the dual-phase steel.

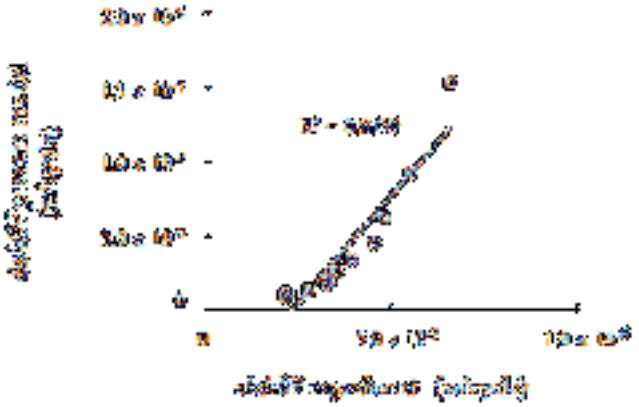

Fig. 9 Linear correlation between predicted FCG rate using present model and calculated FCG rate from experimental data for as-received steel.

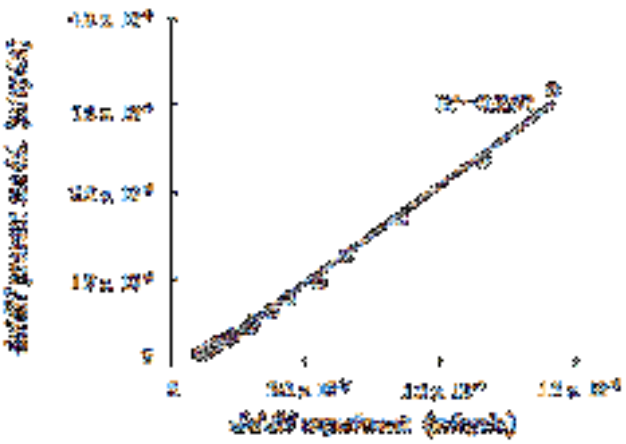

Fig. 10 Linear correlation between predicted FCG rate using present model and calculated FCG rate from experimental data for dual-phase steel.

## 5. Summary

This study demonstrated the concept concerning the understanding of entropy generation in dual-phase steel for the entire FCG test. A temperature evolution was implemented to express the entropy generation in the dual-phase steel through the FCG using the concept of the DEG theorem. Therefore, an FCG model was developed to evaluate the FCG rate based on the DEG theorem. This theorem verified that the crack growth and entropy generation were related by means of the degradation coefficient to ensure that the empirical Paris-Erdogan law of crack growth could simply be observed from an evaluation of the DEG theorem. The results proved that the present model was able to accurately predict the experimental results, particularly for the dual-phase steel, which was definitely closer to $\Delta K^4$ with an RMSE value of 7.3471 x $10^{-7}$. Thus, according to the results, the present model does seem to be acceptable for various metals, especially those presenting a $\Delta K^4$ that is dependent on the fatigue crack growth rate. Moreover, the results of the present model were sensitive to differences in the FCG mechanism as a result of different microstructures with a regression value, $R^2$ of 0.9952.

## References


[1] Basaran, C., and Yan, C.Y. A thermodynamic framework for damage mechanics of solder joints. *J. Elect. Pack*., Volume 120, (1998), pp. 379-384.

[2] Thamburaja, P., and Jamshidian, M. A multiscale Taylor model-based constitutive theory describing grain growth in polycrystalline cubic metals. *J. Mech. Phys. Solids*, Volume 63, (2014), pp. 1-28.

[3] Jamshidian, M., Thamburaja, P., and Rabczuk, T. A multiscale coupled finite-element and phase-field framework to modeling stressed grain growth in polycrystalline thin films. *J. Comp. Phys*., Volume 327, (2016), pp. 779-798.

[4] Klamecki, B.E. A thermodynamic model of friction. *Wear*, Volume 63(1), (1980), pp. 113–120.

[5] Naderi, M., and Khonsari, M.M. An experimental approach to low-cycle fatigue damage based on thermodynamic entropy. *Int. J. Solids Struct*, Volume 47(6), (2010), pp. 875–880.

[6] Naderi, M., Amiri, M., and Khonsari, M.M. On the thermodynamic entropy of fatigue fracture, in *Proc. R. Soc. London, Ser. A*, Volume 466(2114), (2009), pp. 423–438.

[7] Chudnovsky, A. Crack layer theory. Univ., Cleveland, OH, Case Western Reserve, NASA Contractor Rep. 174634, (1984).

[8] Ondracek J, and Materna A. FEM evaluation of the dissipated energy in front of a crack tip under 2D mixed mode loading condition. *Proc. Mater. Sci.* (2014), pp. 673–678.

[9] Ahmad Zaidi, A.M., Md Asif, M.M., Abdul Rahman, I., Rasool Mohideen, S., Ahmad Zaidi, A.F., Ahmad Zaidi, N.H., and Yusof, M.S. Finite element simulation on crack analysis of a thick-tube. International Journal of Integrated Engineering, Volume 1, (2009), pp. 67-71.

[10] Naderi, M., and Khonsari, M.M. A comprehensive fatigue failure criterion based on thermodynamic approach. *J. Compos. Mater.* Volume 46(4), (2011), pp. 437-447.

[11] Amiri, M. and Modarres, M. An Entropy-Based Damage Characterization. *Entropy,* Volume 16, (2014), pp. 6434–6463.

[12] Bryant, M.D., Khonsari, M.M., and Ling, F.F. On the thermodynamics of degradation, *Proceedings of the Royal Society of London. Series A. Mathematical, Physical and Engineering Sciences*, Volume 464, (2008), pp. 2001–2014.

[13] Klingbeil, N.W. A total dissipated energy theory of fatigue crack growth in ductile solids. *Int. J. Fatigue*, Volume 25, (2003), pp. 117–128.

[14] Li, S.C., Kang, Y.L., and Kuang, S. Effects of microstructure on fatigue crack growth behaviour in cold-rolled dual phase steels. *Mater. Sci. Eng. A*, Volume 612, (2014), pp. 153–161.

[15] Tang, Y., Zhu, G., Kang, Y., Yue, L., Jiao, X. Effect of microstructure on the fatigue crack growth behavior of Cu-Be-Co-Ni alloy. *J. Alloys Comp*., Volume 663, (2016), pp. 784-795.

[16] Maletta, C., Bruno, L., Corigliano, P., Crupi, V. and Guglielmino, E. Crack-tip thermal and mechanical hysteresis in Shape Memory Alloys under fatigue loading, *Mater. Sci. Eng. A*, Volume 616, (2014), 281–287.

[17] Ismail, A.E., Ariffin, A.K., Abdullah, S., and Ghazali, M.J. Finite element analysis of J-integral for surface cracks in round bars under combined mode I loading. International Journal of Integrated Engineering, Volume 9, (2017), pp. 1-8.

[18] Kumar, A., Singh, S.B, and Ray, K.K. Influence of bainite/martensite content on the tensile properties of low carbon dual phase steels. *Mater. Sci. Eng. A*, Volume 474(1), (2008), pp. 270-282.

[19] Maruyama, K., Sawada, K., and Koike, J.I. Strengthening mechanisms of creep resistant tempered martensitic steel. *ISIJ international*, Volume 41(6), (2001), pp. 641-653.